

Chemical enrichment by Wolf–Rayet and asymptotic giant branch stars

Lynnette M. Dray,¹★ Christopher A. Tout,¹ Amanda I. Karakas²
and John C. Lattanzio²

¹Institute of Astronomy, Madingley Road, Cambridge CB3 0HA

²Department of Mathematics and Statistics, Monash University, Clayton, Victoria 3168, Australia

Accepted 2002 October 3. Received 2002 September 10; in original form 2001 December 18

ABSTRACT

We present theoretical models of Wolf–Rayet (WR) stars for two different sets of mass-loss rates. We compare with observed properties of WR stars and discuss implications for the enrichment of the interstellar medium in both cases. Sets of stellar yields for these stars together with corresponding yields from new models of asymptotic giant branch (AGB) stars are presented and discussed. We find carbon enrichment from WR stars to be on a level comparable to or greater than that from AGB stars for most scenarios. The models predict well the surface abundances and number ratios of WR stars but a population of binaries is needed if the models are to reproduce simultaneously both the observed mass-loss rates and positions on the Hertzsprung–Russell diagram.

Key words: stars: abundances – stars: AGB and post-AGB – stars: Wolf–Rayet.

1 INTRODUCTION

Wolf–Rayet (WR) stars have long been recognized as a potentially important source of chemical enrichment of the interstellar medium (ISM, Chiosi & Maeder 1986). They are thought to originate from the most massive stars – stars of initial mass greater than approximately $25 M_{\odot}$ – which have extremely strong radiation-driven stellar winds and high mass-loss rates.

Owing to this mass loss, the hydrogen envelope of a WR star is stripped away, leaving He and CNO elements which were processed in the interior of the star at the surface. Initially this process leaves the surface composed primarily of He and some remaining H, with enhanced N – the so-called WNL stars. If all the remaining H is stripped away the stars enter the WNE phase and, as mass loss continues, further layers of the star are stripped away to leave a WC star with surface significantly enriched in C and O (Schild & Maeder 1984; Smith & Maeder 1991). WO stars were introduced by Barlow & Hummer (1982) to explain a small number of stars even further enriched in O than WC stars. These appear to be a natural progression from WC stars into a short final phase of WR evolution. The WR types may be divided into a range of further subtypes that are thought to correspond to stages on different evolutionary tracks and with different initial metallicities (Smith & Maeder 1991), though this has been called into question (Crowther et al. 2002).

Over the entire lifetime of a WR star, depending on the initial conditions, most of the mass of the star may be returned to the ISM in the wind. Much of the matter lost in the early stages of evolution is unprocessed but in the later stages, after the envelope has been lost, the wind is highly enriched in He, C and O. This represents one

of the few scenarios in which a star can return partially processed matter to the ISM.

The final supernova (SN) of such a star is likely to be of type Ib or Ic and will also contribute to the CNO enrichment (Ensmann & Woosley 1988) unless the matter given off during the supernova is consumed by the formation of a black hole (BH) (Maeder 1992). Recent observations (Weiler, Panagia & Montes 2001) have supported the theory that gamma-ray bursts (GRBs) are produced by the final SNe of WR stars. Since evolved WR stars are frequently surrounded by ring nebulae of matter thrown off during the evolution, looking for the signature of the interaction of the GRB with the ring nebula could shed some light both on GRBs and on WR stars (Ramirez-Ruiz et al. 2001).

The evolutionary path of a WR star is primarily determined by its initial mass and by the mass-loss rates throughout its evolution; these are the main factors taken into account in this paper. Metallicity, in particular, has a strong effect on the evolution by changing the mass-loss rates (Maeder 1992) and its effects will be looked at in a forthcoming paper. Here we consider only solar metallicity. There are several other factors that are likely to play a part in theoretically reproducing the observed sample of WR stars, for example rotation (Maeder & Meynet 2000) and evolution in a binary system (De Loore & Vanbeveren 1994).

Whilst WR stars are found preferentially in high-metallicity environments, owing to the effect of metals in increasing the opacity in the outer layers of the star and hence the radiative mass loss, some WR stars have been observed at very low metallicity, for example in I Zw 18 (Legrand et al. 1997), which is at a metallicity of 1/50 of the solar value.

About 39 per cent of the WR stars in the solar neighbourhood are or are suspected to be in binaries (van der Hucht 2001); indeed, it is likely that some lower-mass WR stars formed as a result of the effects

★E-mail: ldray@ast.cam.ac.uk

of binary mass transfer only and would have evolved differently had they been single stars. In low-metallicity environments it is possible that binary mass transfer may be required for WR stars to form at all. However, a reasonable fit for the WR population of I Zw 18 has been obtained using single-star models (De Mello et al. 1998).

One of the important features of WR stars is their role in enriching the ISM with carbon. It is still a matter of debate as to how much C originates from WR stars as opposed to type II SNe (Woosley & Weaver 1995) and third dredge-up on the asymptotic giant branch (AGB) (Frost & Lattanzio 1996). Type Ia SNe may also produce a small amount of CNO elements (Matteucci & Greggio 1986). Current models (Maeder 1992; Portinari, Chiosi & Bressan 1998; Maeder & Meynet 1994) indicate that WR stars are the main source of C in the ISM but these models make use of mass-loss rates that take no account of clumped winds and thus are probably overestimates (Crowther 2001). Observationally, the abundance analyses of Gustafsson et al. (1999) and Hou, Prantzos & Boissier (2000) suggest that Galactic carbon is primarily from massive stars. However, Timmes, Woosley & Weaver (1995) find the current main source of carbon to be stars with $M < 8 M_{\odot}$. Kobulnicky & Skillman (1998) find correlation between C/O and N/O ratios, suggesting that production of C and N is coupled and both originate from lower-mass stars. Overviews of the wide range of available studies suggest that no consensus has been reached as to the most important source of carbon (Liang, Zhao & Shi 2001).

The WR stellar models presented in this paper were computed both with the mass-loss rates of Maeder & Meynet (1994) and with the more recent empirical WR mass-loss rates of Nugis & Lamers (2000). We test whether the observations can be reproduced without resort to increasing the mass loss and investigate what effects this has on the enrichment in CNO elements produced by a generation of WR stars.

AGB stars, on the other hand, have long been recognized as an important source of, in particular, C enrichment. Although the amount of carbon produced per star is not particularly large, they do benefit from the shape of the IMF producing large numbers of lower-mass stars. The earliest attempt to calculate their contribution to galactic chemical evolution was the work of Iben & Truran (1978), although yields were explicitly calculated by Renzini & Voli (1981). This has been updated by various authors recently. However, all of these calculations have used synthetic evolutionary calculations to simulate masses with different dredge-up laws, mass-loss formulae, etc. (Marigo, Bressan & Chiosi 1996, 1998; Marigo 2001; van den Hoek & Groenewegen 1997; Forestini & Charbonnel 1997). We have taken a different approach and are in the process of calculating detailed evolution for masses between 1 and $6 M_{\odot}$ and for various compositions, initially for $Z = 0.004, 0.008$ and 0.02 (Lattanzio, Karakas & Pols 2002). These are complete calculations, from pre-zero-age main sequence to the end of the thermally pulsing evolution and include an extensive nucleosynthesis network as well (Lattanzio et al. 2000). It is the yields for the $Z = 0.02$ models which we include here and compare with the WR star yields.

2 STELLAR MODELS

We describe our WR and AGB models separately.

2.1 Wolf-Rayet stars

The computational simulations were carried out using the stellar evolution code first developed by Eggleton (1971), and which has

subsequently been much updated (see Pols et al. 1998 and references therein) to take account of advances in the input physics and application to different stellar evolution problems. Mass loss, necessarily the main feature in constructing models of Wolf-Rayet stars, is easily incorporated in the code. This represents the first systematic application of this code to WR stars. A convective overshooting parameter $\delta_{ov} = 0.12$ is used (for details of the convective overshooting prescription see Schröder, Pols & Eggleton 1997). This value is obtained from comparison of models with varying degrees of overshooting to observations of late-type giants undergoing central helium burning (Schröder et al. 1997). In practice this leads to an overshooting length $l_{ov} \approx 0.2\text{--}0.3 H_p$, which is slightly higher than other massive star models (e.g. Maeder 1992 use $l_{ov} = 0.2 H_p$). We use the reaction rates of Caughlan & Fowler (1988), apart from ^{12}C (α, γ) ^{16}O for which we take the rate of Caughlan et al. (1985). Stars with initial main-sequence masses of $\sim 10\text{--}180 M_{\odot}$ were evolved for both mass-loss rates and the evolution was followed to the end of central carbon burning.

Stars were classified, as in Maeder & Meynet (1994), as WNL stars when their surface H abundance dropped below 0.4 and effective temperature $T_{\text{eff}} > 4.0$, as WNE stars when the surface H dropped to zero, as WC stars when in addition the surface ratio $(\text{C} + \text{O})/\text{He} > 3.0 \times 10^{-2}$ and as WO stars when $(\text{C} + \text{O})/\text{He} > 1.0$.

The first set of models (hereinafter referred to as MM) were evolved using the enhanced mass-loss rates of Maeder & Meynet (1994). These take the empirical mass-loss rates of De Jager, Nieuwenhuijzen & van der Hucht (1988), multiplied by a factor of 2, for the pre-WR evolution, a constant rate of $8 \times 10^{-5} M_{\odot} \text{ yr}^{-1}$ for the WNL phase (doubled with respect to the rate of $4 \times 10^{-5} M_{\odot} \text{ yr}^{-1}$ from Conti 1988), and the theoretical mass-loss rate of Langer (1989) for the later stages, for which

$$\dot{M}_{\text{WR}} = (0.6\text{--}1.0) \times 10^{-7} (M_{\text{WR}}/M_{\odot})^{5/2} M_{\odot} \text{ yr}^{-1}. \quad (1)$$

The models presented here are not identical to Maeder & Meynet's (1994) models because of differences in the code, most notably the different treatment of convective overshooting.

The second set of models (hereinafter referred to as NL) were evolved using the De Jager et al. (1988) mass-loss rates for pre-WR stars (i.e. half the pre-WR mass-loss rate of the MM models) and the empirical mass-loss rates of Nugis & Lamers (2000) for WN and WC stars:

$$\log(\dot{M}_{\text{WN}}) = -13.6 + 1.63 \log L/L_{\odot} + 2.22 \log Y \quad (2)$$

$$\log(\dot{M}_{\text{WC}}) = -8.3 + 0.84 \log L/L_{\odot} + 2.04 \log Y + 1.04 \log Z. \quad (3)$$

These mass-loss rates were chosen to bear as close a resemblance to observed values as possible from the set of empirical formulae available (Crowther 2001). Whilst the authors suggest that the NL WC mass-loss rate is likely to be suitable for the short WO phase too, in practice use of this rate caused problems with numerical stability for some models and we used a constant value of $1.9 \times 10^{-5} M_{\odot} \text{ yr}^{-1}$ instead.

It has been noted (Talon et al. 1997) that the effects of convective overshooting are similar to those of rotationally induced mixing in massive stars and hence these models may also be considered as models with a smaller degree of overshooting but with rotation. However, it should be noted that the effects of rotation and overshooting on surface abundances and yields are not the same (Maeder & Meynet 2001).

A further complication is that the stars closest to the lower-mass limits for WR formation undergo a phenomenon similar to core breathing pulses when the convective boundary crosses the He-burning shell during the early WNL phase. Convective mixing from above the burning shell to below it causes replenishment of He which in turn causes the burning shell to drop back below the convective boundary for a short period before crossing it again. Up to 10 such oscillations typically occur in affected models. Breathing pulses are more commonly seen close to He exhaustion in models of AGB and HB stars (Sweigart 1991) and opinion is divided as to whether they are a real effect or merely numerical in origin (Cassisi et al. 2001). The pulses in our models occur during He shell burning rather than in the core but otherwise their behaviour is similar to that of core pulses.

We find that the breathing pulses may be suppressed by slightly reducing the amount of convective overshooting during the period in which the models are susceptible to pulses and models with and without pulses are included in the enrichment considerations in cases where the suppression of pulses produces a noticeable difference.

2.1.1 WR binaries

In addition to the single-star models, we evolved a number of WR stars in close binary systems. Our binary simulations use a simple extension of the single-star code in which the evolution of the secondary is followed only by varying its mass. Whilst the behaviour of WR binaries is complex and depends on many parameters, our aim here is not to perform a full analysis but instead to check whether the general behaviour of models with binary-related mass transfer is such that adding binaries to our sample of single stars would improve the fit to observations. With this in mind, we consider only the areas of binary parameter space in which complications, such as colliding winds or the secondary itself becoming a WR star in the lifetime of the primary, are least likely to occur – in particular, we use secondaries of up to 10 solar masses only. The mass lost by a single $10 M_{\odot}$ star up to the age when Roche lobe overflow occurs in the binary models we consider here is less than $10^{-2} M_{\odot}$. Since this is negligible compared with other sources of mass transfer and the exact computation of the mass loss requires full computation of the evolution of the secondary, we ignore secondary mass loss in these models. We do, however, include the effects of Bondi–Hoyle wind accretion (Hurley, Tout & Pols 2002) and Roche lobe overflow.

As our current binary models are not suitable for much of the parameter space required for a full investigation of their effect on the WR populations, we include only a small number of models here for comparison with the single stars.

2.1.2 Supernovae

Enrichment comparisons between WR and AGB stars are incomplete if the final supernovae of the WR stars are not considered. The final SNe of WR stars are expected to be of type Ib (no hydrogen observed in the spectrum) or Ic (no hydrogen or helium). Observations of SNe that change from II to Ib over time (Fillipenko & Matheson 1993) and detection of helium in type Ic SNe (Matheson et al. 2000) suggest that there is probably a continuum between all three types determined by the composition of the outer layers of the star. To estimate the amount of supernova enrichment is complicated and strongly depends on assumptions concerning what happens during the supernova. In particular, a black hole may be formed which swallows all the potential SN enrichment (Maeder 1992). SN enrichment thus depends critically on the mass limit for BH formation

as well as the composition of the pre-SN remnant. Core-collapse simulations (Fryer 1999) show that SN progenitors (with no pre-SN mass loss) more massive than $40 M_{\odot}$ may form black holes directly with no SN explosion. In this case, all enrichment from the SN is lost. Furthermore, black holes may form after a SN in the mass range 20 – $40 M_{\odot}$. Chemical evolutionary synthesis models (De Donder & Vanbeveren 2002) suggest that a few solar masses of C and O may be released. Since our models undergo mass loss, it is more meaningful to set a boundary for BH formation based on the mass of the CO core and we consider the enrichment from various boundary scenarios in Section 4.

Extensive simulations of SNe for massive stars with constant mass have been performed by Woosley & Weaver (1995). As shown by Portinari et al. (1998), it is possible to link Woosley & Weaver's total SN yields to the yield that would be produced by the explosion of the central CO core alone, by subtracting contributions from the outer layers of the star. If we take the CO core masses of our stars at the end of their lifetimes we can relate these masses to the CO core masses in the Woosley & Weaver models at the time of SN explosion and use the relation worked out by Portinari et al. to estimate the enrichment. Our stars continue to undergo mass loss even after their CO cores are revealed so it is possible that their final composition may be different from those in the Woosley & Weaver models. Therefore, we calculate the enrichment that would be obtained by peeling off the outer layers of our final models (in an onion skin manner) down to the remnant masses given by the comparison with Woosley & Weaver. In this case we also need to consider any processing that may have occurred between the end of central C burning, when we finished evolving our models, and the SN. The most important effect is likely to be the pre-supernova destruction of C. The effect the actual explosion has on C and O abundances is small (Imbriani et al. 2001). The purpose of our onion-skin calculation is to check the accuracy of applying Woosley & Weaver SNe to our models, so we only check that the onion skin C enrichment is greater than our SN C enrichment and use the amount of O enrichment to compare the two SN assumptions more closely.

2.2 AGB stars

Evolutionary calculations were performed with the Monash version of the Mt Stromlo Evolution Code, updated to include OPAL opacity tables of Iglesias & Rogers (1996). Nucleosynthesis is then calculated with a modified version of the code used by Cannon (1993), with updated nuclear reaction rates as given by Lugaro (1998). Note that we do not use any overshoot in the convective zones, in the usual sense. The only extent of mixing is our search for a neutral Schwarzschild convective boundary, as outlined in Frost & Lattanzio (1996). This is totally negligible in the context of convective core burning in the masses considered, but it may have an effect on the depth of third dredge-up, as discussed in detail in Frost & Lattanzio (1996).

We include mass loss according to the Reimers formula on the first giant branch, with $\eta = 0.4$, and on the AGB we use the formulation of Vassiliadis & Wood (1993). For consistency with the calculations of Frost (1997) we do not include the modification to the mass-loss rate for masses above $2.5 M_{\odot}$ as suggested by Vassiliadis & Wood (1993) to account for long-period optically visible variable stars.

2.3 IMF

When considering the stellar population as a whole we need to assume an initial mass function (IMF). A power-law function

$\xi(m) \propto m^\gamma$ is usually adopted, for which the ‘slope’ is $\Gamma = d \log \xi(\log m) / d \log m$. It is generally accepted that a single value of Γ is appropriate for the whole range of massive (greater than $8 M_\odot$) stars and there is evidence that the IMF is remarkably uniform despite different star-forming conditions (Kroupa 2002). The exact value of Γ quoted, however, varies – Kroupa, Tout & Gilmore (1993) find $\Gamma = -1.7$, whereas the more recent study of Massey (1998) finds a less steep value of $\Gamma = -1.3$, which is close to the Salpeter value of -1.35 (Salpeter 1955). Kroupa (2002) supports the use of $\Gamma = -1.3$ but also notes that, if the fraction of stars in binaries which are not resolved from their more massive companions is considered, a value of $\Gamma = -1.7$ may be more appropriate (Sagar & Richtler 1991). This difference in Γ may significantly alter the amount of enrichment coming from the upper end of the mass range and so we consider both IMF slopes for calculations where an IMF is required. Since we use the full mass range of our input models to represent the WR population we have also effectively imposed an IMF upper-mass cut-off at around $150 M_\odot$. However, the huge early mass loss and relative scarcity of stars close to this mass limit is such that the CNO enrichment they produce is very small indeed. The lowering of the upper cut-off mass to, for example, $120 M_\odot$ would therefore make little difference to the properties of the WR population, at least at solar metallicity.

3 COMPARISON WITH OBSERVATIONS

To test their suitability we compare our WR models with four distinct observable quantities.

3.1 Mass limits

For WR stars of solar metallicity we observe three distinct evolutionary paths for which the initial mass limits are given in Table 1. Stars at the lower end of the mass range (M_{low} to M_{wc}) undergo a brief WNL phase after the red supergiant (RSG) phase and before core collapse. Between M_{wc} and M_{up} stars go through a RSG phase before entering the WN phase, but then proceed with their evolution through WC to a short final WO phase. Models with initial mass above M_{up} have high enough mass-loss rates that the stars do not undergo a RSG phase, but become WN stars, whilst still in the blue region of the Hertzsprung–Russell (HR) diagram. The most massive of these stars finish their evolution in the WC phase. It is notable that these mass limits are surprisingly similar, given the large difference (a factor of 2–4, depending on the evolutionary phase) in mass-loss rate used. Observational evidence for the actual limits at which different types of evolution occur may be gathered from cluster turn-off studies (Schild & Maeder 1984). Massey, DeGioia-Eastwood & Waterhouse (2001) find that galactic WN stars may have progenitor masses as low as $25 M_\odot$ and higher than $120 M_\odot$, a range which fits well with the theoretical values, particularly when it is considered that the theoretical lower-mass limit (M_{low}) is likely to be lowered slightly by the inclusion of binary evolution and rotation. Whilst the same study finds M_{wc} to be $70 M_\odot$, this is based on a very small sample of WC stars. A rather lower M_{wc} ($45 M_\odot$) has

been found for the Magellanic Clouds which, as systems of lower metallicity, would be expected to have a M_{wc} greater than that in the Milky Way. This indicates that it is likely that the real solar-metallicity mass limit is much lower and the anomaly is caused by the sample size.

There exist a number of earlier cluster turn-off mass studies: Humphreys, Nichols & Massey (1985) find a lower limit for WR formation of $30 M_\odot$ and that 80 per cent of WR stars have initial masses greater than $50 M_\odot$. Schild & Maeder (1984), in contrast, find a lower limit of $18 M_\odot$. However, as noted by Massey, Waterhouse & DeGioia-Eastwood (2000), the above percentages are likely to have large error bars as these studies relied on earlier results in which a number of high-mass stars were missed or misclassified. For our models we find only around 47 per cent of our WR stars (MM or NL) are initially above $50 M_\odot$, assuming a constant SFR and the IMF of Kroupa et al. (1993). 80 per cent of our WR stars are initially above $34 M_\odot$.

3.2 Number ratios

Number ratios of different WR subtypes are another observational test that can be applied to the theoretical models. Table 2 shows the observed subtype ratios in comparison with the number ratios predicted at solar metallicity for different values of the IMF slope. For the purpose of this analysis, an O star is one with a surface temperature greater than 33000 K.

Whilst the ratios are reasonably close to the observed value, both sets of models overproduce WO stars and underproduce WNE stars. Although the observed WO population consists of a handful of stars and hence statistically cannot be used in meaningful number ratio comparisons, the WO population from our models may be as much as half of the WC population – a situation far from reality! Since an observed star is classified as a WO star on the basis of relative spectral line strengths rather than surface composition as in our models, it is possible that some of our WO stars are misclassified WC stars. In this case, the WC/WR and WC/WN ratios increase, whilst the other ratios quoted in Table 2 remain constant.

The lack of WNE stars is seen at solar metallicity but is more pronounced at lower metallicities where the theoretical proportion of WNE stars declines towards zero but the observed proportion increases. As noted by Maeder & Meynet (1994), a possible explanation is that at low metallicity the proportion of WR stars that have formed via binary-related mass loss is greater. To test this, we evolve a number of binary stars as detailed in Section 2.1.1 with parameters typical of observed WR binaries (van der Hucht 2001 and references therein). Whilst our binary models are simple and the real situation is likely to be far more complicated, these models provide a useful indication of the general trend of WR or pre-WR star behaviour likely to result from a period of Roche lobe overflow. Table 3 shows the time spent in the different WR phases for single stars and for

Table 2. WR subtype ratios for observed and theoretical populations of WR stars distributed with IMF slope Γ and a constant SFR.

	WR/O	WN/WR	WNE/WR	WC/WR	WC/WN
Obs	0.10	0.52	0.10	0.48	0.92
$\Gamma = -1.7$					
MM	0.08	0.34	0.07	0.46	1.37
NL	0.05	0.43	0.05	0.33	0.76
$\Gamma = -1.3$					
MM	0.11	0.41	0.08	0.44	1.07
NL	0.06	0.46	0.05	0.32	0.69

Table 3. Time spent in different WR phases for single stars and stars in binaries.

Model	Primary	Secondary	Period	$t_{\text{pre-WR}}$	t_{WNL}	t_{WNE}	t_{WC}	t_{WO}
NL	22 M_{\odot}	–	–	8.5×10^6 yr	0 yr	0 yr	0 yr	0 yr
NL	22	10 M_{\odot}	20 d	7.8×10^6	8.0×10^5	2.7×10^4	0	0
MM	22	–	–	8.7×10^6	0	0	0	0
MM	22	10	20	7.9×10^6	3.6×10^4	7.0×10^5	6.1×10^5	0
NL	31	–	–	5.9×10^6	1.3×10^5	2.1×10^3	9.5×10^4	2.8×10^4
NL	31	10	10	5.7×10^6	2.6×10^5	1.9×10^5	1.7×10^5	2.9×10^4
NL	31	10	20	5.6×10^6	2.3×10^5	1.5×10^5	1.7×10^5	7.1×10^4
MM	31	–	–	5.8×10^6	3.1×10^4	8.6×10^3	2.9×10^5	1.7×10^5
MM	31	10	10	5.8×10^6	4.0×10^4	2.4×10^5	6.1×10^5	0
MM	31	10	20	5.7×10^6	3.9×10^4	1.9×10^5	6.0×10^5	0
NL	40	–	–	4.6×10^6	1.6×10^5	0	1.2×10^5	1.6×10^5
NL	40	10	20	4.5×10^6	2.8×10^4	9.3×10^4	1.8×10^5	1.4×10^5
MM	40	–	–	4.7×10^6	5.4×10^4	2.8×10^4	3.0×10^5	1.9×10^5
MM	40	10	20	4.6×10^6	1.7×10^5	4.0×10^5	5.9×10^5	0

binaries with a range of primary masses and initial periods. For all models the time spent in the WNE period is increased by orders of magnitude by the effects of a period of Roche lobe overflow. The MM binaries also have a shortened or absent WO phase. The same is not true of the NL models, which have a similar or increased WO phase. However, this phase generally comprises a smaller fraction of the total WR phase.

These effects are caused by high mass loss from Roche lobe overflow early in the evolution. As a result, the He core is revealed at an earlier stage. After mass transfer the remaining mass of the WR star is often considerably less than that of the corresponding single star, which leads to lower mass-loss rates during the WNE phase. These factors increase the WNE lifespan and, since the lower mass loss continues throughout the WC phase, it discourages the onset of a WO phase.

The total time in the WR phase is increased by a factor of 2–3 and the mass limit for WR formation is lowered. As the IMF strongly favours lower-mass stars in this mass range, these factors indicate that the influence of WR binaries on the total WR population is likely to be significant even if binaries initially form a relatively small proportion of the stellar population. This effect will be more pronounced at lower metallicity, where the mass threshold for single WR star formation is higher.

3.3 Positions in the HR diagram

Combined modelling of WR interior structure and atmosphere (Schaerer 1996) shows that, whilst the interior structure of the star is unaffected by the atmospheric conditions, external parameters of the star, such as the effective temperature, are likely to be strongly affected by them. In the light of this analysis, straightforward comparisons of HR diagram positions with observation are not accurate and other quantities that depend less on atmospheric structure need to be considered instead. Surface abundances are suitable here – commonly used comparisons are between luminosity and H or He abundance for WN stars and luminosity and (C + O)/He for WC stars (Langer et al. 1994; Maeder & Meynet 1994). These are shown in Figs 1 and 2. Overlaid are observational values for WR stars from Koesterke & Hamann (1995) and Hamann & Koesterke (1998) and luminous OB stars from Herrero et al. (1992). From Fig. 1 we see that our WN stars have a good fit to the observations. The MM models fit the observed WNE star luminosities more accurately than the NL models, but for the WNL both mass-loss rates fit observations rather well. It should be noted that our classifica-

tion methods assume that any star with surface H mass fraction greater than 0.4 is not a WR star; this condition would need to be altered to fit the few WR stars in this sample with surface H greater than this. A couple of binary star tracks (primary mass 31 M_{\odot} , secondary mass 10 M_{\odot} and initial periods 10 and 20 d) are included for each set of models. It can be seen that the fit is improved in both cases. Observations of WR stars thought to be in binaries are overlaid as diamonds (Hamann & Koesterke 1998; van der Hucht 2001). These show that the WR binary population is spread out widely in luminosity and H abundance. WR 87, at luminosity 6.3, is the only star that we have trouble explaining, even when binaries are included. If the NL mass-loss rates are assumed, it could potentially be a star with high initial mass (greater than 90 M_{\odot}) in a non-interacting binary.

In Fig. 2 we plot the mass fraction ratio C/(C + He) against the luminosity, because the observed values from Hamann & Koesterke (1995) for WC stars do not include O. Also plotted are the Galactic WC stars from Crowther et al. (2002). The Hamann & Koesterke calculations of the mass fractions assume a pure helium–carbon composition and hence are less suitable for the more extreme WC and WO stars in which oxygen becomes a significant fraction of the surface abundance. The results of the WC star comparison are, in fact, very similar to those obtained less accurately by plotting the HR diagram tracks. For the single WC stars, a good fit is obtained for the MM models, but the majority of the NL models are at too great a luminosity. This may indicate a requirement for an extra source of mass loss at some earlier point in the evolution – for example, a specific high mass-loss LBV phase is not included here (see, e.g., Langer et al. 1994), but the inclusion of one would tend to shift the following evolutionary phases towards lower mass and lower luminosity. There is no such requirement for the MM models. As with the WN phase, we also plot on Fig. 2 a couple of binary star tracks (parameters as before). For the MM models, these tracks are essentially similar to those of single stars with higher initial mass than the initial primary mass. For the NL stars we see that the inclusion of close binaries significantly improves the fit to observations of our models. However, many of the stars in the region of the graph covered by the binary models but not the single stars have not been found to be in binaries.

3.4 Surface abundances

Comparison of theoretical and observed surface abundance ranges from Nugis (1991) (Table 4) show good agreement in both cases, in

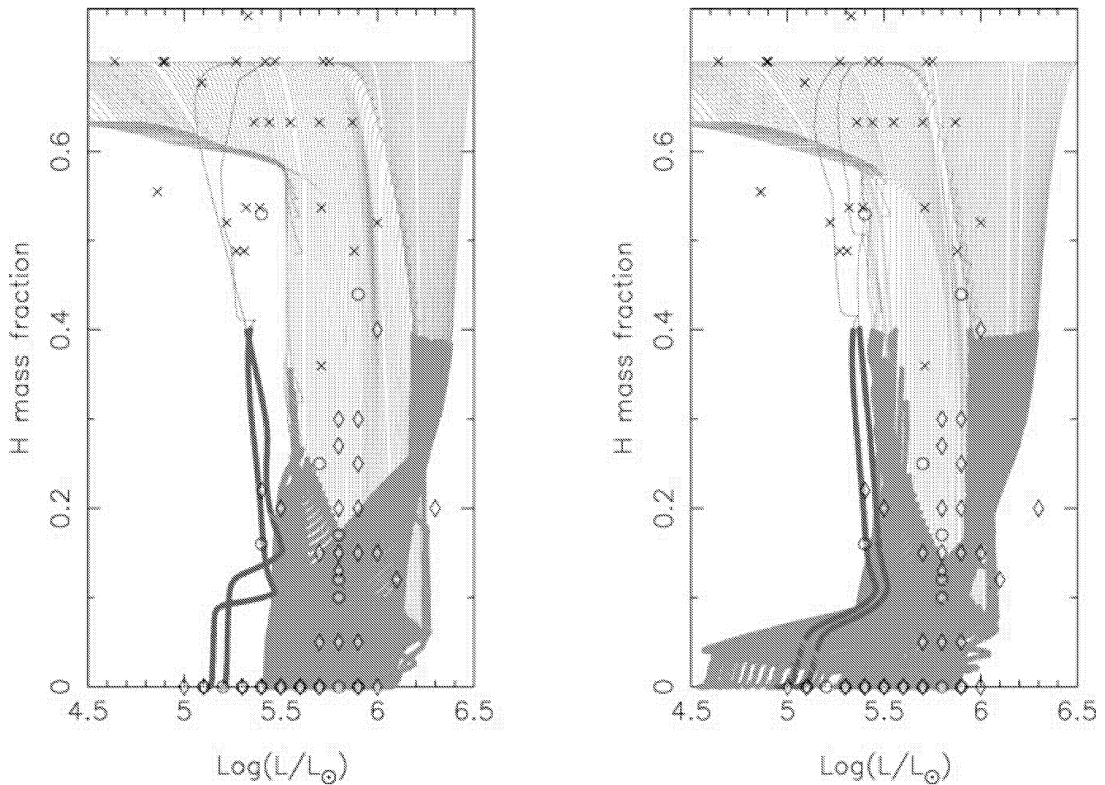


Figure 1. Comparison of theoretical and observed positions of WN stars in the $\log(L/L_{\odot})$ versus surface H plane. Left: NL models. Right: MM models. Tracks of pre-WR OB stars are shown by thin grey lines and those of WN stars by thick grey lines. Overlaid are observational values for OB stars from Herrero et al. (1992) (crosses) and for single WN stars (circles) and WN stars thought to be in binaries (diamonds) from Hamann & Koesterke (1998). We also include a couple of binary star tracks (black, see the text for parameters).

part because the different WR phases were defined by their effect on surface abundance in the models. The greatest uncertainty lies at the extremes of C and O abundances, caused by the uncertain mass-loss conditions at the very end of the WR lifetime. WO stars are included in the figures for WC stars.

4 ENRICHMENT

The enrichment from a single WR star is sensitive to the mass-loss rates and their variation throughout the evolution of the star. The more massive stars lose much of their mass as H and He before further processing to CNO elements has taken place, whereas stars at the lower threshold for WR formation have cores that are already highly evolved when they are exposed but lose less of this evolved material in the wind. For our models we find that, whilst individual interactions between mass-loss rate and enrichment in different evolutionary phases may be quite complex, the total enrichment from a complete WR population is much less sensitive to our assumed mass-loss rates than might be expected.

For each WR star evolved we have calculated the total amount of wind enrichment in CNO (filled circles in Fig. 4). In the left-hand panels of Fig. 4 the IMF of Kroupa et al. 1993 ($\Gamma = -1.7$) is applied to the yields and scaled such that the area under the curve is proportional to the total yield. Similarly in the right-hand panels of Fig. 4 we apply the IMF supported by Massey (1998) ($\Gamma = -1.3$) to our yields.

The AGB star yields are given in Table 5 and the WR star yields in Tables 6 and 7.

We do not include our sample of binary WR stars, since they only cover a small region of the parameter space occupied by a full population of binaries. Enrichment from the WR primary is rather lower than for a single star, but much of the difference is in H and He transferred to the secondary. A full enrichment analysis would thus also require consideration of the evolution of the secondary and what happens to it during and after the final SN of the primary, which is beyond the scope of this paper.

We also consider the SN enrichment as described in Section 2.1.2. Analysis of the widths of light curves of type Ib supernovae (Ensmann & Woosley 1988) suggests that observed type Ib supernovae may be constrained to masses between 4 and $7 M_{\odot}$. In addition, they must retain some of their helium layer but have lost all of their hydrogen layer. Type Ic SN display an absence of both hydrogen and helium in their spectra: Crowther et al. (2002) suggest for Galactic type Ic SN final masses in the range $7\text{--}14 M_{\odot}$. The final mass distribution of the theoretical models as given in Tables 6 and 7 (M_{sn}) and Fig. 3 shows that most of the MM models that become WR stars fall within the $4\text{--}7 M_{\odot}$ mass range, but the NL models have final masses concentrated in the range $7\text{--}20 M_{\odot}$. The pre-SN models have a range of surface He abundances with models with lower final mass generally having higher final surface He. This is because these models, whether by having a lower initial mass or by undergoing very high mass loss early in their evolution, enter the WNE phase at a relatively low mass. Subsequent mass loss, which acts to strip the outer He layer, is then small. From these surface abundances we would expect the more massive remnants to undergo type Ic SNe and the less massive ones to undergo type Ib SNe as indicated

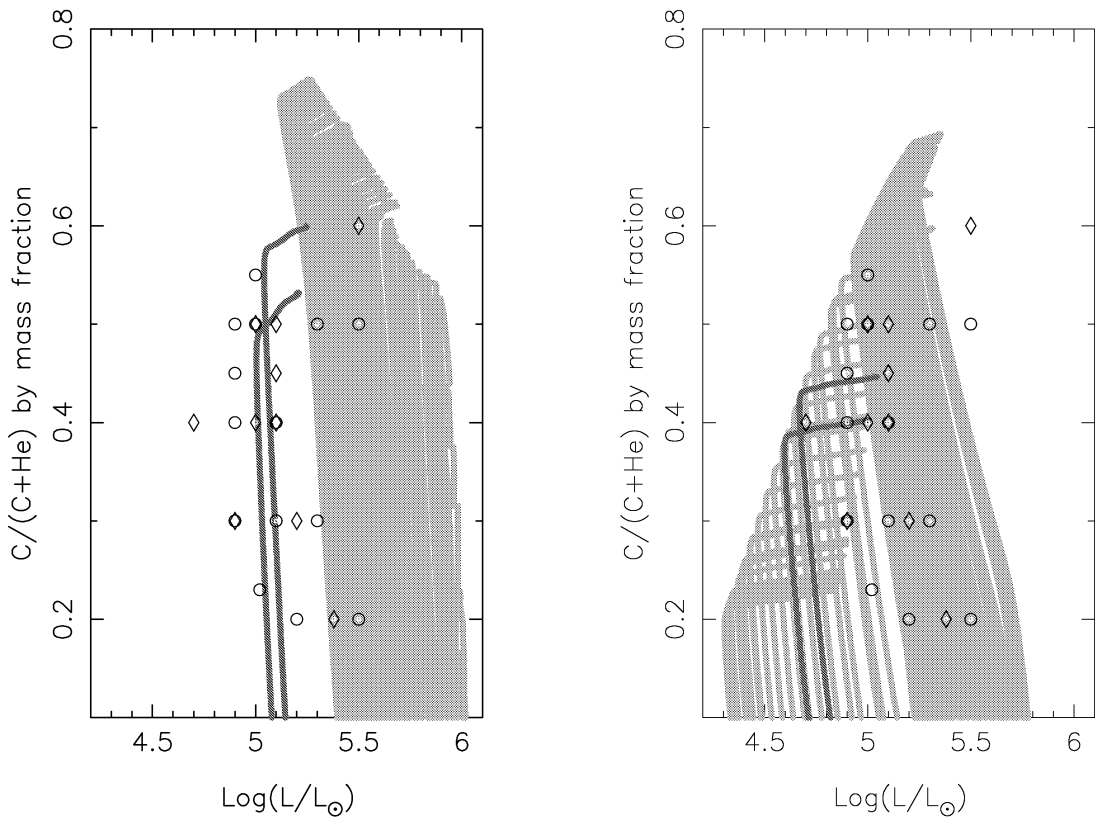


Figure 2. Comparison of theoretical and observed positions of WC stars in the $\log(L/L_{\odot})$ versus $C/(C + \text{He})$ plane. Left: NL models. Right: MM models. Theoretical tracks are shown in grey. Observational values (circles) are from Hamann & Koesterke (1995) and Crowther et al. (2002).

Table 4. WR surface abundance ranges for solar metallicity.

Model	Subtype	$N(\text{He})/N(\text{H})$	$N(\text{N})/N(\text{He})$	$N(\text{C})/N(\text{He})$	$N(\text{O})/N(\text{He})$
Observed	WN	0.7–10	0.01–0.003	≤ 0.004	–
MM	WN	$0.36-\infty$	0.034–0.002	0.073–0.000 06	0.044–0.000 07
NL	WN	$0.36-\infty$	0.032–0.002	0.0178–0.000 06	0.032–0.000 07
observed	WC	≥ 10	–	0.7–0.1	0.05–0.02
MM	WC	∞	0.027–0	0.743–0.008	0.437–0.0002
NL	WC	∞	0.032–0	0.996–0.007	0.783–0.0002

above. It is likely from our final masses that the reality is somewhere between the two sets of mass-loss rates. This would favour the NL rates since most of the factors left unconsidered in this analysis (e.g. rotation and binarity) act to lower rather than raise the final mass.

We plot the total (wind and SN) enrichment in Figs 3 and 4 as open circles, in the case that the vast majority of stars produce enrichment from the final SN.

In Tables 6 and 7 we also include the onion-skin O enrichment obtained with the assumption that all matter in our final pre-SN model external to the SN remnant is ejected with no processing during the SN for comparison with the Woosley & Weaver CO core mass SN O yields. If our use of the Woosley & Weaver yields is justified the two sets of O yields should be similar. The onion-skin yields are shown in Fig. 4 (crosses). We find the yields to be very close, particularly for the MM models. A high pre-SN mass is the main source of discrepancy between the two but such

SNe are the most likely to produce no enrichment through BH formation.

As a further check, we verified that our onion-skin C enrichment was less than the Woosley & Weaver C values, as C is likely to be destroyed in the period between which we finish detailed evolution of our models and ejection into the ISM.

We must also consider the case in which black hole formation swallows all enrichment from stars with a final CO core mass above $M_{\text{CO},\text{max}}$ (Maeder 1992). In Figs 4 and 5 the effect of this is to remove the SN enrichment (open circles) for WR models with a pre-SN mass (given by Tables 6 and 7) greater than the threshold. Carbon is primarily ejected in the wind and is little affected by reductions in the SN enrichment. However, the WR oxygen yield becomes much smaller when the SN yield is removed. SNe of stars below the mass limit for WR formation, which have smaller final CO cores than most of the WR stars and so are less affected by the mass cut-off, are strongly favoured as oxygen sources by the slope

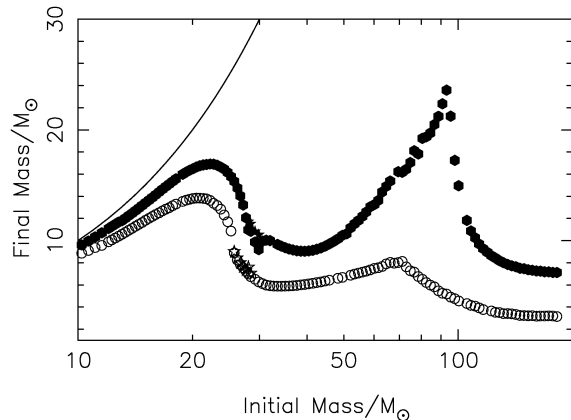


Figure 3. Final (pre-supernova) masses of WR stars as a function of initial mass. Open points: MM models. Closed points: NL models. Star-shaped points indicate models in which breathing pulses were suppressed. The solid line is for no mass loss.

of the IMF and are still the main source of oxygen even when no cut-off is applied.

Table 8 shows the enrichment produced when one solar mass of initially solar-composition matter is processed by WR stars with various values of $M_{\text{CO,max}}$. As can be seen from Fig. 3, there is only a small overlap between the NL WR final mass distribution and that of the MM models. We therefore calculate the enrichment for NL models with $M_{\text{CO,max}}$ of 12, 10 and 8, and for the MM models 8 and 6, as no MM WR models have M_{CO} above $10 M_{\odot}$ and no NL WR models have M_{CO} below $6 M_{\odot}$. Comparison of the scenarios in Table 8 confirms that, over the whole distribution of WR stars, carbon is little affected by a SN mass cut-off but oxygen may be reduced by a factor of 3 or more. The other main effect of the cut-off is, unsurprisingly, to increase the proportion of the initial matter which is not returned to the ISM. The IMF chosen makes little difference to the quantities in Table 8 as they are relative to the total amount of WR enrichment.

Comparing our carbon yields with those from other massive star models (Fig. 5, top), we note that the MM rates agree well with Portinari et al. (1998). In particular, our total enrichment integrated over the whole population of WR stars is very similar to that of Portinari. Our agreement with Maeder is poorer but the differences seem to be a matter of scale rather than the shape of the curve and stem from the greater total mass lost in the wind that Maeder's WR models undergo. The NL models give worse agreement, particularly in the range $50-80 M_{\odot}$, where the final mass is large enough that much of the carbon created in the stars is never ejected.

All the studies find the peak mass for WR carbon enrichment to be near the threshold mass for WR formation; for our MM models this peak is at a slightly lower value than for Maeder and Portinari. This is because of our greater level of overshooting tending to increase the mass loss and hence shift the behaviour of stars near the boundary mass for WR formation towards the behaviour of stars with greater initial mass. Similarly the decrease in C enrichment at $80-100 M_{\odot}$ caused by the transition from evolution with a RSG phase to evolution with no RSG phase begins at a slightly lower mass for our models. There is a peak around the transition point that is more pronounced with the $\Gamma = -1.3$ IMF.

We note that our SN ^{12}C yields at the lower end of the mass range are rather high compared with those of other studies. This is

caused by the effect of our high overshooting increasing the mass of the final CO core over a mass range for which the amount of C enrichment is quite sensitive to the core mass (Portinari et al. 1998). For comparison, our initially $12 M_{\odot}$ star has a final CO core of $2.6 M_{\odot}$, whereas the corresponding star of Woosley & Weaver (1995) has one of $1.8 M_{\odot}$ and that of Maeder (1992) has $2.1 M_{\odot}$.

A similar comparison for oxygen enrichment (Fig. 4, bottom) shows that the final supernova is particularly significant in increasing O yields. Our models are very close in O enrichment to the other massive star models, particularly to those of Portinari. There is little difference between the MM and NL models over most of the mass range, though our NL models show a slightly higher oxygen yield for initial masses $40 < M_i/M_{\odot} < 60$. This is caused by the intermediate to high remnant masses of these models and is very sensitive to $M_{\text{CO,max}}$.

With the exception of the small number of stars that end their evolution in the WN phase, the WR models had final nitrogen abundances of zero and hence the final SN does nothing to enhance the already small amount of N produced. Nitrogen enrichment from the WR wind is shown in the centre panel of Fig. 5; the relatively large amount from stars below the mass threshold for WR formation and from AGB stars confirms that at solar metallicity massive stars play an insignificant role in N enrichment in comparison with intermediate-mass stars. Our agreement with Portinari et al. is good, though we have a small rise in N enrichment above approximately $90 M_{\odot}$. This only appears to a much lesser degree in their yields. It may be a consequence of greater resolution and different mass-loss rate assumptions.

Some comments on the yields for low-mass stars are appropriate. Note that the yields from van den Hoek & Groenewegen (1997) and Marigo (2001) are the results for synthetic calculations, where the detailed hydrostatic structure and evolution is not calculated. Rather the results of detailed models are parametrized in terms of major variables (e.g. the H exhausted core mass), including approximations for dredge-up and the interpulse period, etc. The models we present are the result of full hydrostatic evolutionary sequences. They are thus more likely to be correct, although a known problem exists with predictions of ^{12}C at low masses (see below). We will discuss ^{12}C and ^{14}N only; the yields for ^{16}O are negligible.

First, we note that the ^{12}C yields from our models are substantially lower than those from either of the synthetic calculations. This is because those calculations have been fitted to the C star luminosity function observed in the Magellanic Clouds. One of the benefits of synthetic models is that, because they use simple parametrizations to model the structure of TP-AGB stars, one can perform rapid population synthesis and quickly determine the effects of variations in, say, the internal evolution or prescriptions for mass loss, etc. It is well known that detailed evolutionary models do not predict enough C stars at low luminosities and this is adjusted within synthetic calculations by adjusting the dredge-up parametrizations until a fit is obtained. This usually involves beginning the dredge-up at lower luminosities (and hence core masses) than found in detailed models.

It is not clear that such a procedure means that the synthetic models are more reliable at predictions other than the C star distribution, however. The constraint is rather simple: it is not even the C/O ratio that is constrained, but rather simply the binary value of 'yes' for C/O > 1 or 'no' for C/O < 1. Much more information exists in both the data and models and a thorough confrontation between models and theory, for many species, still remains to be made. This is likely

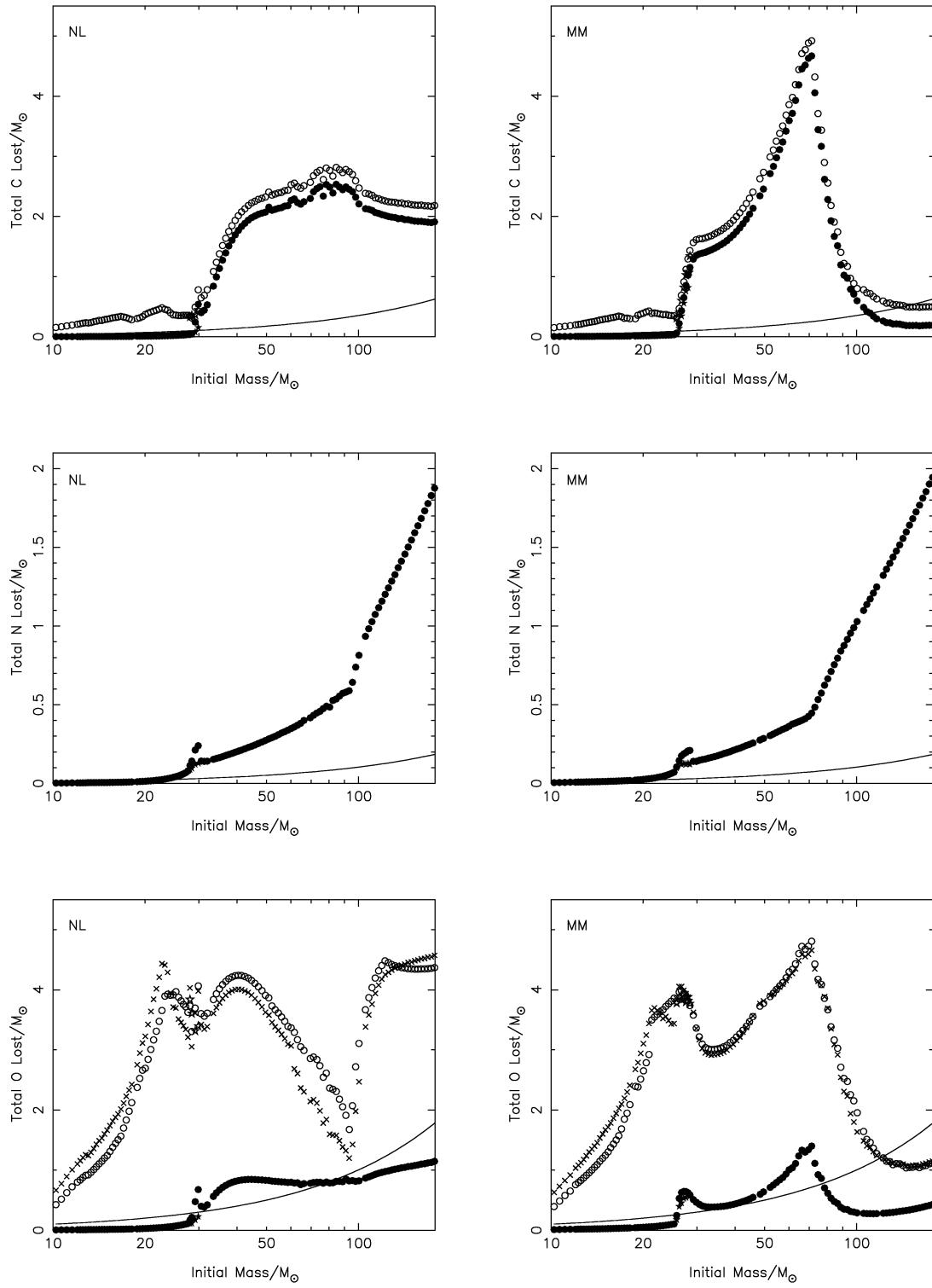


Figure 4. Total CNO expelled by WR stars for our MM and NL models. Filled points indicate wind enrichment only; open ones wind + SN. Star-shaped points indicate those models in which breathing pulses were suppressed. Solid lines indicate the amounts present in the models before evolution. For O, we also include wind plus onion-skin SN enrichment (crosses).

to provide much more information concerning the changes required to bring the models into agreement with observations, rather than simple changes to the dredge-up parametrization. Nevertheless, the dredge-up in the synthetic models has been adjusted to give more ^{12}C earlier and this is why the yields are higher. Whether such a

procedure produces more reliable yields, especially for other species, is unknown.

Note that, once the mass exceeds $3 M_\odot$, the agreement is very good. This is because the modifications to produce the lower-luminosity C stars are all made for low masses. Note also that the

Table 5. $Z = 0.02$ AGB star yields in CNO elements.

M_i	^{12}C	^{13}C	^{14}C	^{14}N	^{15}N	^{16}O	^{17}O	^{18}O
1.25	-0.776E-03	0.354E-04	0.768E-27	0.376E-03	-0.102E-05	-0.999E-03	0.843E-06	-0.186E-05
1.5	-0.122E-02	0.456E-04	0.210E-26	0.721E-03	-0.164E-05	-0.134E-02	0.301E-05	-0.370E-05
1.75	-0.168E-02	0.591E-04	0.201E-26	0.107E-02	-0.228E-05	-0.168E-02	0.860E-05	-0.553E-05
1.9	-0.185E-02	0.626E-04	0.664E-25	0.117E-02	-0.252E-05	-0.189E-02	0.125E-04	-0.625E-05
2.25	-0.113E-02	0.705E-04	0.699E-10	0.160E-02	-0.312E-05	-0.255E-02	0.431E-04	-0.825E-05
2.5	0.177E-02	0.796E-04	0.473E-09	0.199E-02	-0.367E-05	-0.311E-02	0.378E-04	-0.997E-05
3.0	0.973E-02	0.983E-04	0.102E-07	0.267E-02	-0.480E-05	-0.433E-02	0.430E-04	-0.135E-04
3.5	0.158E-01	0.112E-03	0.399E-08	0.344E-02	-0.602E-05	-0.562E-02	0.419E-04	-0.173E-04
4.0	0.689E-02	0.154E-03	0.260E-08	0.420E-02	-0.734E-05	-0.611E-02	0.448E-04	-0.198E-04
5.0	-0.979E-03	0.181E-02	0.136E-08	0.146E-01	-0.165E-04	-0.929E-02	0.324E-04	-0.888E-04
6.0	-0.114E-01	0.528E-03	0.531E-09	0.353E-01	-0.195E-04	-0.153E-01	0.643E-04	-0.109E-03

parameters determined by matching the Magellanic Cloud C-star distributions are then used at other compositions.

^{14}N is more complicated. First, we notice that the synthetic models of Marigo agree very well with our detailed calculations. In view of the previous paragraph, this may be surprising. However, the AGB has a negligible effect on ^{14}N in low-mass stars: there is no second dredge-up, (almost) no ^{14}N is dredged to the surface during third dredge-up and there is no hot-bottom burning. So the main source of ^{14}N in low-mass stars is the first dredge-up. Hence adjusting the parameters for the third dredge-up should have a negligible effect on the ^{14}N yields for low masses and this is seen in Fig. 5. The rapid increase in the ^{14}N yields at 4 M_\odot reflects the initiation of hot-bottom burning. The agreement between Marigo and our work is excellent.

The agreement with van den Hoek & Groenewegen is good at high masses but poorer for lower masses. They show a slightly increasing ^{14}N yield as M decreases from 4 to 1 M_\odot , which seems to reflect mostly the initial mass function. The higher ^{14}N yield for low masses may be caused by their starting with more N and C (destined to become N) than we do.

For comparison with the WR and AGB yields presented here we include on the IMF-weighted plots (Fig. 5) the yields of Marigo (2001), van den Hoek & Groenewegen (1997), Maeder (1992) and Portinari et al. (1998). SN II yields from Woosley & Weaver (1995) between 11 and 25 M_\odot are also shown in these plots; these do not include pre-SN mass loss but the mass loss of models in this range is generally small.

The effect of the assumed IMF on the relative proportions of carbon produced by the different classes of stars is large. If the steeper IMF is used (left-hand panels), both our MM and NL models produce an amount of carbon that is comparable to that produced by AGB stars. Using the AGB yields presented here, WR stars remain the greater source of carbon but if the yields of Marigo (2001) are considered instead the enrichment from both sources is nearly equal. In general, comparison of yields from a range of AGB and massive star models as in Fig. 5 leads to the conclusion that most combinations of solar metallicity AGB and WR models will be slightly but not strongly dominated by the WR yields. It is also interesting to note that our large final CO cores for stars in the mass range 10 – 20 M_\odot lead to a not insignificant amount of SN II C enrichment.

On the other hand, use of the less steep IMF (right-hand panels) leads to WR yields that are always greater than those from AGB stars, even if the Marigo AGB yields are used. If we use the AGB results presented in this paper, the shallower IMF slope leads to WR stars being the strongly dominant source of carbon.

Overall, our results for carbon fall roughly in between those of other studies – for most combinations of yields, IMF and SN conditions, we find that massive stars play a slightly less important role in its production (at least at solar metallicity) than suggested by Gustafsson et al. (1999) and Hou et al. (2000) but a more important role than found by Timmes et al. (1995).

A similar comparison for nitrogen leads to the conclusion that AGB stars, particularly those in the mass range 4 – 8 M_\odot are the principal source of N at solar metallicity – the same conclusion reached by the chemical evolution models of Henry, Edmunds & Köppen (2000) and Timmes et al. (1995). It should be noted, however, that the effects of rotation in massive stars may increase the N yield (Meynet & Maeder 2000). It is also interesting to note that using $\Gamma = -1.3$ the nitrogen contribution of massive stars is large enough to be potentially significant.

We also find, as expected from many chemical evolution models (e.g. Prantzos, Vangioni-Flam & Chauveau 1994; Hou et al. 2000; Timmes et al. 1995, etc.) that oxygen yields are dominated by stars above 10 M_\odot . The question of the relative importance of the WR stars and non-WR stars in this mass range is more interesting, but cannot be answered without a more thorough understanding of which stars proceed to black hole formation. If we consider the extreme scenarios, WR and non-WR massive stars contribute roughly equally to O enrichment in the case where $M_{\text{CO},\text{max}}$ is high enough for no solar metallicity WR stars to form black holes. If $M_{\text{CO},\text{max}}$ is low (perhaps around 4 M_\odot) then SNe of stars with initial mass 10 – 25 M_\odot dominate. The most noticeable difference between our MM and NL models occurs at intermediate values of $M_{\text{CO},\text{max}}$. If it is set at 7 M_\odot then the MM models produce significant amounts of O but the NL models produce almost none.

Yields of H, He, C, N and O are given in Tables 5–7. M_i is the initial main-sequence mass of the star. M_{sn} is the final pre-SN mass of the star, and M_f is the mass remaining post-SN. A suffix ‘w’ denotes wind enrichment alone; one of ‘ws’ denotes combined wind and SN enrichment. O_{onion} indicates the O yield when the amount of O in the onion-skin layers of our pre-SN remnant external to the final remnant mass is assumed to be our SN yield and is included for comparison with the SN yields obtained from the CO cores of Woosley & Weaver (1995).

Yields of an element are defined here, as in Tinsley (1980) and modified in Maeder (1992), to be the mass fraction of a star that is converted to the element and returned to the ISM during the entire lifetime of the star, hence

$$E_{iM} = (M - M_f) X_i^0 + M p_{iM}, \quad (4)$$

where E_{iM} is the total amount of species i ejected by a star of initial mass M (in solar masses) and final mass M_f with initial i abundance

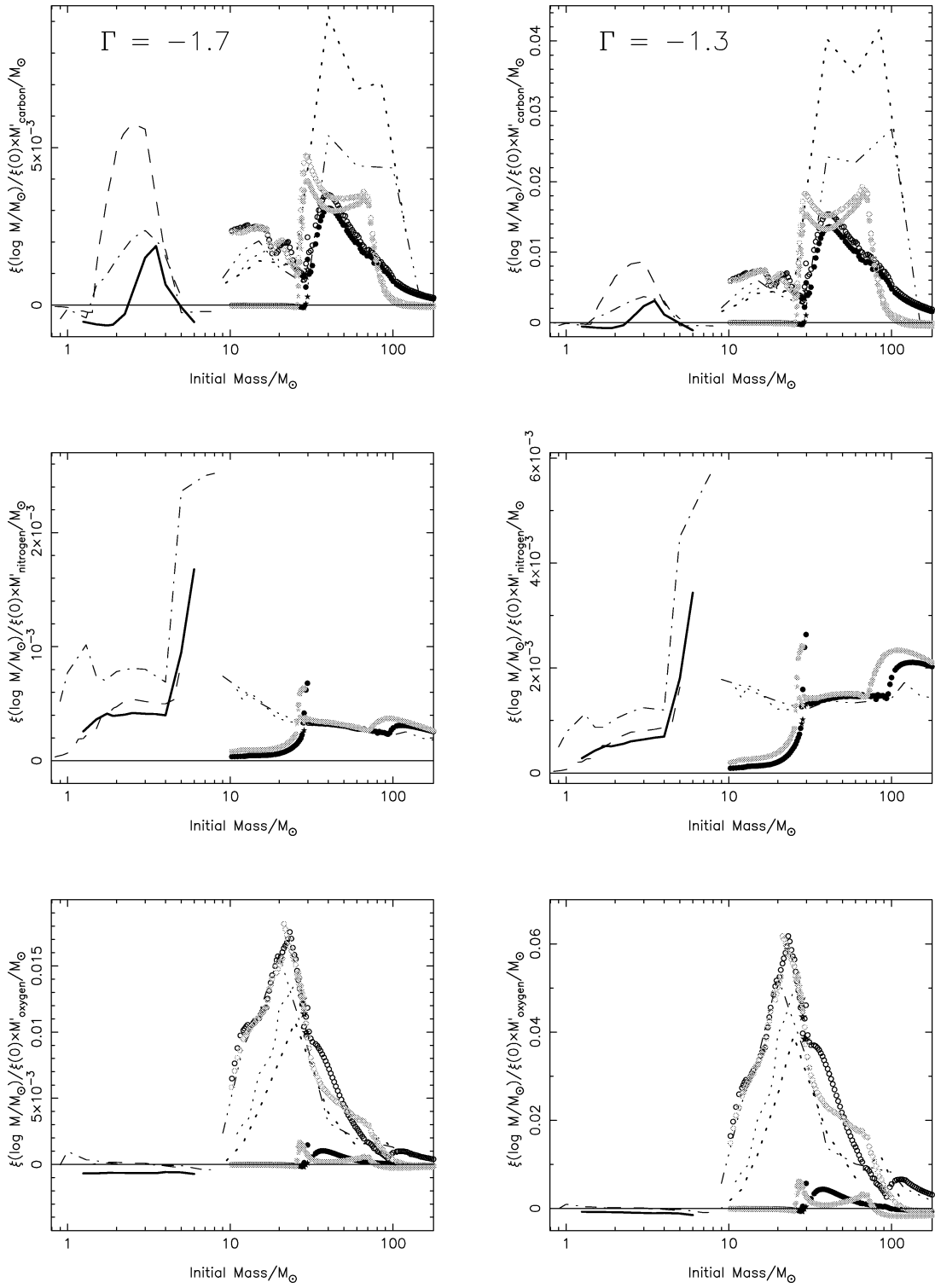


Figure 5. CNO enrichment from WR stars, AGB stars and type II SNe, weighted by IMFs $\xi(x)$ of slope $\Gamma = -1.7$ and -1.3 , where M'_x is the mass of element X ejected by the star minus the amount that would have been ejected had no processing occurred. Points for the WR stars are as in Fig. 4, with MM shown models in grey and NL models in black. The AGB yields presented here are shown by the solid bold line. For comparison, we also show AGB yields from Marigo (2001) (dashed line) and van den Hoek & Groenewegen (1997) (dot-dashed line), massive star yields from Maeder (1992) (bold dotted line) and Portinari et al. (1998) (dot-dot-dashed line) and SN II yields from Woosley & Weaver (1995) (dotted line).

Table 8. Mass fractions of elements produced by processing 1 solar mass of matter at various metallicities in WR stars.

Model	$M_{\text{CO},\text{max}}$	H	He	C	N	O	Ne	Remnant
Initial model	–	0.7	0.28	0.004	0.001	0.010	0.002	–
$\Gamma = -1.7$								
MM (wind)	–	0.324	0.476	0.034	0.007	0.011	0.004	0.141
MM (wind+SN)	∞	0.324	0.483	0.039	0.007	0.072	0.004	0.050
NL (wind)	–	0.302	0.427	0.029	0.006	0.013	0.003	0.217
NL (wind+SN)	∞	0.302	0.434	0.034	0.006	0.071	0.003	0.141
NL (wind+SN)	12	0.302	0.432	0.032	0.006	0.063	0.003	0.153
NL (wind+SN)	10	0.302	0.430	0.031	0.006	0.047	0.003	0.172
MM (wind+SN)	8	0.324	0.480	0.039	0.007	0.062	0.004	0.065
NL (wind+SN)	8	0.302	0.428	0.029	0.006	0.016	0.003	0.212
MM (wind+SN)	6	0.324	0.478	0.036	0.007	0.027	0.004	0.116
$\Gamma = -1.3$								
MM (wind)	–	0.324	0.496	0.032	0.007	0.010	0.004	0.124
MM (wind+SN)	∞	0.324	0.503	0.037	0.007	0.064	0.004	0.044
NL (wind)	–	0.301	0.446	0.028	0.007	0.013	0.003	0.201
NL (wind+SN)	∞	0.301	0.451	0.032	0.007	0.064	0.003	0.133
NL (wind+SN)	12	0.301	0.449	0.031	0.007	0.055	0.003	0.145
NL (wind+SN)	10	0.301	0.448	0.030	0.007	0.042	0.003	0.162
MM (wind+SN)	8	0.324	0.501	0.036	0.007	0.056	0.004	0.056
NL (wind+SN)	8	0.301	0.446	0.028	0.007	0.016	0.003	0.195
MM (wind+SN)	6	0.324	0.498	0.033	0.007	0.025	0.004	0.101

X_i^0 , and p_{iM} is the yield. We then calculate the wind enrichment using

$$Mp_{iM} = \int_0^{\tau_M} \dot{M}(M, t) [X_i^s(t) - X_i^0] dt, \quad (5)$$

where X_i^s is the surface abundance of i at time t and τ_M is the lifetime of the star. The values Mp_{iM} are quoted in Tables 5–7. Lines prefixed with an ‘s’ indicate models in which breathing pulses were suppressed.

5 CONCLUSIONS

(i) The solar-metallicity WR models presented here are generally in good agreement with observations. The most notable deviation is in the positions of WC stars with NL mass-loss rates in the luminosity–surface composition diagram, with observations fitting the MM models much more closely. However, the inclusion of a realistic proportion of binary stars could solve this problem.

(ii) Changes in the mass-loss rate, even by a factor of 2 or more, have only a small effect on the total yields over the WR population of different elements. Hence, unless the actual mass-loss rates of WR stars are very different from those used here, we are confident that our carbon and nitrogen yields are close to the actual values. The O enrichment is less certain, as it depends strongly on whether a BH is formed in the final SN.

(iii) We find that WR stars play an important part in carbon enrichment of the ISM at solar metallicity, at a level at least comparable to that of intermediate-mass stars for an IMF slope of $\Gamma = -1.7$ and dominant for an IMF slope of $\Gamma = -1.3$. Enrichment by N is dominated by AGB stars, whereas O enrichment is dominated by SNe.

ACKNOWLEDGMENTS

LMD acknowledges support from PPARC. CAT thanks Churchill College for a fellowship. JCL and AIK would like to thank the Victorian Partnership for Advanced Computing as well as the Australian Partnership for Advanced Computing for generous alloca-

tions of time and for financial support. This work was completed with the partial assistance of the Australian Research Council. We would also like to thank the anonymous referee for detailed and helpful comments.

REFERENCES

- Barlow M.J., Hummer D.G., 1982, in De Loore C.W.H., Willis A.J., eds, Proc. IAU Symp. 99, Wolf-Rayet Stars, Observations, Physics, Evolution. Reidel, Dordrecht, p. 387
- Cannon R.C., 1993, MNRAS, 263, 817
- Cassisi S., Castellani V., Degl'Innocenti S., Piotto G., Salaris M., 2001, A&A, 366, 578
- Caughlan G.R., Fowler W.A., 1988, At. Data Nucl. Data Tables, 40, 284
- Caughlan G.R., Fowler W.A., Harris M.J., Zimmerman B.A., 1985, At. Data Nucl. Data Tables, 35, 198
- Chiosi C., Maeder A., 1986, ARA&A, 24, 329
- Conti P.S., 1998, in Conti P.S., Underhill A.B., eds, O Stars and Wolf-Rayet Stars, p. 81
- Crowther P.A., 2001, The influence of binaries on stellar population studies, ASSL, 264, 215
- Crowther P.A., Dessart L., Hillier D.J., Abbott J.B., Fullerton A.W., 2002, A&A, 392, 653
- De Donder E., Vanbeveren D., 2002, New Astron., 7, 55
- De Jager C., Nieuwenhuijzen H., van der Hucht K.A., 1988, A&AS, 72, 259
- De Loore C., Vanbeveren D., 1994, A&A, 292, 463
- De Mello D.F., Schaefer D., Heldmann J., Leitherer C., 1998, ApJ, 507, 199
- Eggleton P.P., 1971, MNRAS, 151, 351
- Enzman L., Woosley S., 1988, ApJ, 333, 754
- Fillipenko A.V., Matheson T., 1993, IAU Circ., 5787
- Forestini M., Charbonnel C., 1997, A&AS, 123, 241
- Frost C.A., 1997, PhD thesis, Monash Univ.
- Frost C.A., Lattanzio J.C., 1996, ApJ, 473, 383
- Fryer C.L., 1999, AJ, 522, 413
- Gustafsson B., Karlsson T., Olsson E., Edvardsson B., Ryde N., 1999, A&A, 342, 426
- Hamann W.-R., Koesterke L., 1998, A&A, 333, 251
- Henry R.B.C., Edmunds M.G., Köppen J., 2000, ApJ, 541, 660
- Herrero A., Kudritzki R.P., Vilchez J.M., Kunze D., Butler K., Haser S., 1992, A&A, 261, 209

- Hou J.L., Prantzos N., Boissier S., 2000, 362, 921
 Humphreys R.M., Nichols M., Massey P., 1985, AJ, 90, 101
 Hurley J.R., Tout C.A., Pols O.R., 2002, MNRAS, 329, 897
 Iben I., Jr, Truran J.W., 1978, ApJ, 220, 980
 Iglesias C.A., Rogers F.J., 1996, ApJ, 464, 943
 Imbriani G., Limongi M., Gialanella L., Terrasi F., Straniero O., Chieffi A., 2001, ApJ, 558, 903
 Karakas A.I., Lattanzio J.C., Pols O.R., 2002, preprint (astro-ph/0210053)
 Koesterke L., Hamann W.R., 1995, A&A, 259, 503
 Kroupa P., 2002, Sci, 295, 82
 Kroupa P., Tout C.A., Gilmore G., 1993, MNRAS, 262, 545
 Kobulnicky H.A., Skillman E.D., 1998, ApJ, 497, 601
 Langer N., 1989, A&A, 220, 135
 Langer N., Hamann W.-R., Lennon M., Najarro F., Pauldrach A.W.A., Puls J., 1994, A&A, 290, 819
 Lattanzio J.C., Frost C.A., Cannon R.C., Wood P.R., 2000, Proc. IAU Symp., 177, 449
 Legrand F., Kunth D., Roy J.-R., Mas-Hesse J.M., Walsh J.R., 1997, A&A, 236, L17
 Liang Y.C., Zhao G., Shi J.R., 2001, A&A, 374, 936
 Lugardo M., 1998, in Prantzos N., Harissopoulos S., eds, Nuclei in the Cosmos, Vol. V. Elsevier, Amsterdam, p. 501
 Maeder A., 1992, A&A, 264, 105
 Maeder A., Meynet G., 1994, A&A, 287, 803
 Maeder A., Meynet G., 2000, ARA&A, 361, 159
 Maeder A., Meynet G., 2001, A&A, 375, 555
 Marigo P., 2001, A&A, 370, 194
 Marigo P., Bressan A., Chiosi C., 1996, A&A, 313, 545
 Marigo P., Bressan A., Chiosi C., 1998, A&A, 331, 564
 Massey P., 1998, in Gilmore G., Howell D., eds, ASP Conf. Ser. Vol. 142, The Stellar Initial Mass Function. Astron. Soc. Pac., San Francisco, p. 17
 Massey P., Waterhouse E., DeGioia-Eastwood K., 2000, AJ, 119, 2214
 Massey P., DeGioia-Eastwood K., Waterhouse E., 2001, AJ, 121, 1050
 Matheson T., Filippenko A., Chornock R., Leonard D.C., Li W., 2000, AJ, 119, 2303
 Matteucci F., Greggio L., 1986, A&A, 154, 279
 Meynet G., Maeder A., 2000, A&A, 361, 101
 Nugis T., 1991, in van der Hucht K., Hidayat B., eds, Proc. IAU Symp. 143, Wolf-Rayet Stars And Interrelations With Other Massive Stars In Galaxies. Kluwer, Dordrecht, p. 75
 Nugis T., Lamers H.J.G.L.M., 2000, A&A, 360, 227
 Pols O.R., Schroder K.-P., Hurley J.R., Tout C.A., Eggleton P.P., 1998, MNRAS, 298, 525
 Portinari L., Chiosi C., Bressan A., 1998, A&A, 334, 505
 Prantzos N., Vangioni-Flam E., Chauveau S., 1994, A&A, 285, 132
 Ramirez-Ruiz E., Dray L.M., Madau P., Tout C.A., 2001, MNRAS, 327, 829
 Renzini A., Voli M., 1981, A&A, 94, 175
 Sagar R., Richtler T., 1991, A&A, 250, 324
 Salpeter E.E., 1955, ApJ, 121, 161
 Schaerer D., 1996, A&A, 309, 129
 Schild H., Maeder A., 1984, A&A, 136, 237
 Schröder K.-P., Pols O.R., Eggleton P.P., 1997, MNRAS, 285, 696
 Smith L.F., Maeder A., 1991, A&A, 241, 77
 Sweigart A.V., 1991, in Janes K., ed., ASP Conf. Ser. Vol. 113, The Formation and Evolution of Star Clusters. Astron. Soc. Pac., San Francisco, p. 299
 Talon S., Zahn J.-P., Maeder A., Meynet G., 1997, A&A, 322, 209
 Tinsley B.M., 1980, Fund. Cosmic Phys., 5, 287
 Timmes F.X., Woosley S.E., Weaver T.A., 1995, ApJS, 98, 617
 Vanbeveren D., De Donder E., Van Bever J., Van Rensbergen W., De Loore C., 1998, New Astron., 3, 443
 van den Hoek L.B., Groenewegen M.A.T., 1997, A&AS, 123, 305
 van der Hucht K.A., 2001, New Astron. Rev., 45, 135
 Vassiliadis E., Wood P.R., 1993, ApJ, 413, 641
 Weiler K.W., Panagia N., Montes M.J., 2001, ApJ, 562, 670
 Woosley S.E., Weaver T.A., 1995, ApJS, 101, 181

This paper has been typeset from a \TeX / \LaTeX file prepared by the author.